ELSEVIER

Journal of Alloys and Compounds 388 (2005) 41–48

Journal of ALLOYS AND COMPOUNDS

www.elsevier.com/locate/jallcom

Microstructural characterisation of Fe–Cr–P–C powder mixture prepared by ball milling

N. Bensebaa[a], S. Alleg[a], F.Z. Bentayeb[a], L. Bessais[b], J.M. Grenèche[c,*]

[a] *Laboratoire de Magnétisme et de Spectroscopie des Solides, Faculté des Sciences, Université de Annaba, B.P. 12, Annaba 23000, Algérie*
[b] *CNRS -Laboratoire de Chimie Métallurgique des Terres Rares–Groupe des Laboratoires de Thiais, 2-8 rue Henri Durant, Thiais Cedex 94320, France*
[c] *Laboratoire de Physique de l'État Condensé - UMR 6087, Université du Maine, 72085, Le Mans Cedex 9, France*

Received 6 May 2004; received in revised form 18 June 2004; accepted 18 June 2004

Abstract

In an attempt to prepare amorphous $Fe_{77}Cr_4P_8C_{11}$ alloy by mechanical alloying, powder mixtures of Fe, Cr, P and C (activated carbon) with a purity of 99.9% have been ball milled, under argon atmosphere for several periods up to 90 h, in a planetary ball mill (Fritsch P7). The structure and microstructure of the milled powders have been characterised, as a function of milling time, by X-ray diffraction and Mössbauer spectrometry. During the first stage of milling (up to 12 h), detailed analyses of the diffraction patterns and the Mössbauer spectra reveal a complete dissolution of the elemental powders and the formation of Fe_xP ($1 < x < 2$), Fe_3P phosphides and Fe_3C carbide in addition to α-(Fe,Cr) phase. The amorphous like state is reached after 32 h of milling. Further milling leads to the appearance of new carbides such as $(Fe,Cr)_7C_3$ and ε'-$Fe_{2.2}C$ with the phosphide $(Fe,Cr)_3P$ type phase embedded in the amorphous matrix.

Keywords: Magnetic properties of nanostructures; Amorphous structure; Mössbauer spectroscopy

1. Introduction

Mechanical alloying (MA) has received a great deal of interest and inspired numerous researches because of its promising results, wide possible application and potential scientific values. It has been used to alloy elemental powders mixture on an atomic scale to form amorphous powders [1–3] or nanocrystalline phases [4,5]. Amorphous materials containing carbon such as Fe–C [6,7], Fe–P–C [8] and Fe–Cr–C [9] have attracted particular attention due to their importance in the steel industry. From the behaviour of the milled Fe–C system [10,11], it has been shown that the resultant product is not governed entirely by the starting composition, but might be affected by numerous milling parameters and milling conditions in the evolution of the reaction products. Thus, Tanaka et al. [10] have carried out an extensive investigation of $Fe_{1-x}C_x$ powders (graphite, $x = 0.17$–0.9) by the use of a conventional ball mill. They have reported that after 2000 h of milling, ferromagnetic carbides such as Fe_3C and Fe_7C_3 were formed when x is ranged from 0.17 to 0.25, and from 0.29 to 0.7, respectively. However, for high carbon content with x ranges from 0.8 to 0.9, fine paramagnetic Fe based particles were also detected. In contrast, Le Caër and Matteazzi [11] have successfully obtained the equivalent phases in the $Fe_{1-x}C_x$ powders (graphite, $0 < x < 0.5$) after milling for only several tens of hours, because of the higher milling energy of the SPEX 8000 ball mill. According to the starting compositions, they observed the formation of FeC alloy and α-Fe for $x < 0.15$; carbides such as Fe_3C and Fe_5C_2 for $0.15 < x < 0.25$ and Fe_7C_3 for $x > 0.3$. Campbell et al. [12] have studied the effects of milling in the $Fe_{75}C_{25}$ powder mixture (both graphite and activated carbon) in vacuum for periods of up to 285 h using a uni-ball mill. They have detected an amorphous Fe_3C-type phase for milling periods of up to 70 h with the crystalline Fe_3C phase formed on further

* Corresponding author. Tel.: +33-243833301; fax: +33-243833518.
E-mail address: greneche@univ-lemans.fr (J.M. Grenèche).

0925-8388/$ – see front matter © 2004 Elsevier B.V. All rights reserved.
doi:10.1016/j.jallcom.2004.06.075

milling time of 140 h. The carbon-rich Fe_7C_3 phase (graphite) was observed on extended milling time up to 285 h. Basset et al. [13] have noted that during milling of Fe–25C powders, the Fe_3C phase was produced after 5 h whereas, a mixture of ε-F_2C and χ-$Fe_{2.5}C$ phases was produced after 10 h. Wang et al. [14] reported that Fe_7C_3 phase was produced on milling an Fe–50C powder mixture for 210 h in a uni-ball mill.

Amorphous (Fe,Cr)–metalloid alloys are currently produced in ribbon form by melt spinning and planar flow [15–17] and studied for their favourable magnetic and mechanical properties which make them potentially useful in many industrial applications [18]. During the last decade, extensive research has been carried out on the mechanical alloying of Fe-based amorphous alloys including binary FeC [10–12], FeZr [19], FeB [20], ternary FeSiB [21] and multicomponents FeNiSiP [22] and FeNiSiB [23], since the nanocrystalline powders produced by MA possess properties which differ from those of systems prepared by conventional techniques. Considering that there are about 10–50% of the atoms located in the grain boundaries, this new solid state manifests considerable changes in physical and mechanical properties. Nevertheless, the amorphisation mechanism by MA is not clearly understood.

The purpose of the present work is to report the alloying process and therefore the formation of an amorphous quaternary alloy with the following composition: $Fe_{77}Cr_4P_8C_{11}$. The process, by which the amorphous state is produced through the structural powder mixture changes, is studied by means of X-ray diffraction (XRD) and ^{57}Fe Mössbauer spectrometry (MS) as a function of milling time.

2. Experimental procedure

A mixture of elemental Fe, Cr, P and C (activated carbon) powders with a purity of 99.9% was performed by the use of a planetary ball mill – Frietsch Pulverisette P7 – with a powder to ball weight ratio of 2/35 and a milling intensity of seven. These milling conditions correspond to a kinetic shock energy and an injected shock power value, respectively, equal to 0.79 J/hit, and 18 W/g.

The structural evolution of the milled powders as well as the phase identification have been followed by XRD measurements using a Siemens D501 diffractometer with Cu Kα radiation (λ = 0.154056 nm). A numerical procedure based on the Rietveld method combined with a Fourier analysis through the Maud program [24] was used to analyse the XRD patterns with broadened peaks, allowing us to obtain several microstructure parameters like, crystallite size, residual micro strains, lattice parameters, phase proportions and preferred orientation. The accuracy of the results is related to the value of the quality factor of fitting, GoF, which is close to unity.

In order to monitor the alloying evolution and to inspect the local interaction between the Fe nuclei as well as to image the nearest neighbourhood of the iron atoms at every stage of the milling process, Mössbauer measurements were applied. Mössbauer spectra, which were taken at room temperature in a transmission geometry using a radioactive ^{57}Co source diffused in a rhodium matrix, were computer fitted using Mosfit [25], a least-square iteration program. The isomer shift is given relative to the centre of the α-Fe spectrum at 300 K. Due to the complexity of the Mössbauer spectra for each milling time, different fitting models were used in order to give a realistic description. Thus, the Mössbauer spectra of the milled Fe, Cr, P and C powders mixture up to 12 h were fitted using: (i) the α-Fe component; (ii) a doublet for the paramagnetic part and (iii) a hyperfine field distribution, HFD, with a linear correlation between the isomer shift and the hyperfine magnetic field for the disordered component. However, the Mössbauer spectrum of the powder milled for 32 h was fitted with only HFD using a linear correlation between the isomer shift and the hyperfine magnetic field. For the powders milled for at least 32 h, the Mössbauer spectra were fitted with a doublet and five magnetic components.

3. Results

XRD patterns were taken for the elemental powder mixture and after each milling time in order to follow the mixing process and the structural changes that occur during ball milling. The XRD patterns of the milled powders (Fig. 1) are found to contain a significant number of overlapping peaks arising from the formation of crystalline intermediate products such as phosphides and carbides. As the milling process progresses, one observes a continuous decrease in the peak heights of the Bragg reflections of the elements, a slight shift of the diffraction peak position and separately the emergence of two extremely broadened peaks centred at about 45° and 80°, in addition to the appearance of new peaks. Those features suggest the formation of a multi-component alloy powder containing nanocrystalline grains having different sizes and structures.

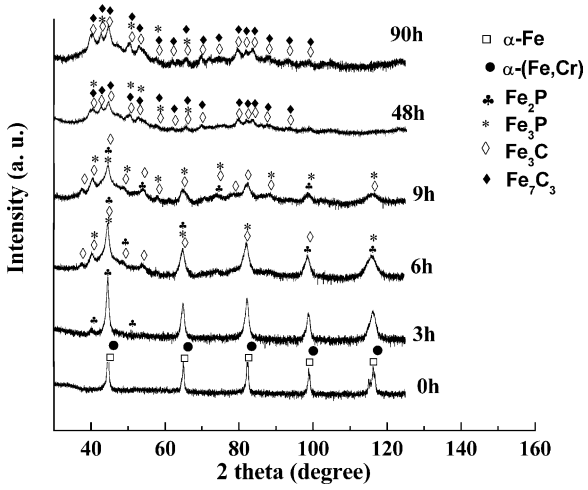

Fig. 1. XRD patterns of the FeCrPC powders as a function of milling time, for 0–90 h.

Table 1
Lattice parameters (a, b, c) and microstructure parameters (L and σ, crystalline grain size and microstrains, respectively) deduced from the fitting of the XRD patterns of the milled powders

Milling time (h)		Phases	a (Å) ($\pm 10^{-3}$)	b (Å) ($\pm 10^{-3}$)	c (Å) ($\pm 10^{-3}$)	L (nm) (± 5)	σ ($\pm 10^{-3}$)
3	Matrix	α-Fe	2.869	–	–	63	3.0
		(Fe,Cr)	2.886	–		26	3.1
	Phosphide	Fe_2P	5.87		3.448	91	3
6	Matrix	α-Fe	2.869	–	–	62	3.1
		(Fe,Cr)	2.875			13	9
	Phosphides	Fe_2P	5.879		3.442	83	9
		Fe_3P	9.187		4.46	127	82
	Carbide	Fe_3C	5.084	6.778	4.547	13	10
9	Matrix	α-Fe	2.874	–	–	45	9.8
		(Fe,Cr)	2.881	–		83	–
	Phosphides	Fe_2P	5.879	–	3.432	7	28
		Fe_3P	9.116	–	4.45	125	87
	Carbide	Fe_3C	5.107	6.769	4.523	7	8
48	Phosphides	$(Fe,Cr)_3P$	9.18	–	4.43	4	10
	Carbides	$(Fe,Cr)_3C$	5.107	6.748	4.476	15	17
		$(Fe,Cr)_7C_3$(hexa)	6.92	-	4.525	16	7
		$(Fe,Cr)_7C_3$(ortho)	9.492	6.889	12.011	13	6
90	Phosphide	$(Fe,Cr)_3P$	9.09		4.457	2	1.9
	Carbides	$(Fe,Cr)_3C$	5.125	6.649	4.514	73	14
		$(Fe,Cr)_7C_3$(hexa)	6.912	–	4.530	12	6.7
		$(Fe,Cr)_7C_3$(ortho)	4.520	6.893	12.018	6	6.9

The change in width at half of maximum of the X-ray peaks as a function of the milling time, gives evidence of the reduction of the particles down to nanometer scale (see Table 1), because of large plastic deformation and repeated fracturing induced during the milling process. Also, high density of defects is generated with prolonged mechanical milling duration leading to an increase in micro-hardness of the powder particles as well as to an increase of internal micro strains (Table 1).

After 3 h of milling, the diffraction pattern is consistent with that of the un-reacted α-Fe, the α-(Fe,Cr) and the phosphide phase where the lattice parameters a = 5.87 Å and c = 3.448 Å, are close to those of the hexagonal Fe_2P phase [26]. After 6 h of milling, one observes the appearance of new diffraction peaks related to phosphides and carbides. The lattice parameters of the new phosphide phase are a = 9.187 Å and c = 4.46 Å instead of a = 9.107 Å and c = 4.46 Å for the tetragonal Fe_3P phase [27] while those of the carbide a =

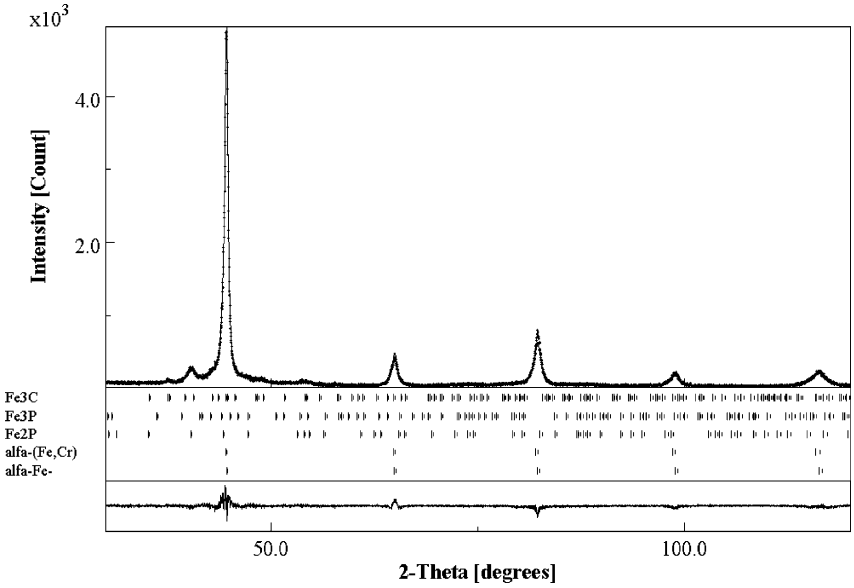

Fig. 2. Fitted XRD pattern of the FeCrPC powder milled for 6 h.

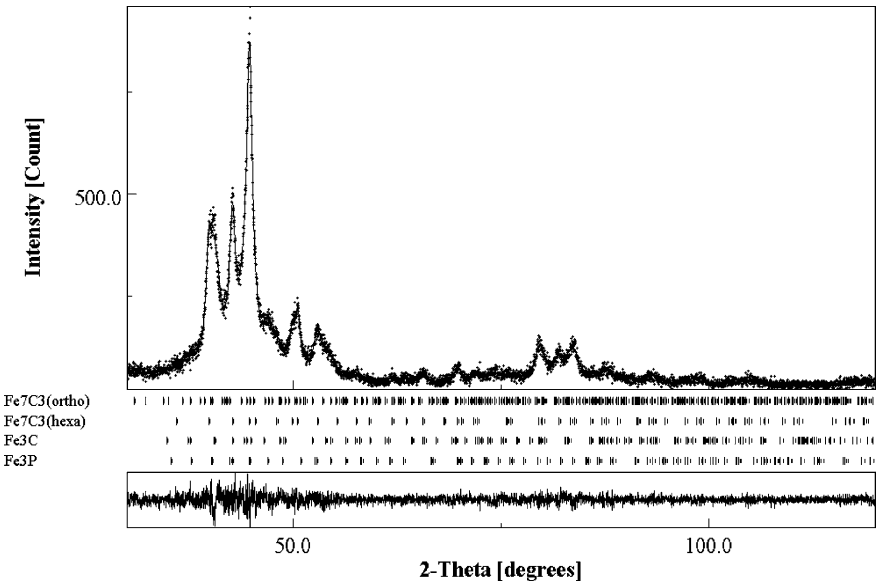

Fig. 3. Fitted XRD pattern of the FeCrPC powder milled for 90 h.

5.0837 Å, b = 6.778 Å and c = 4.547 Å are close to those of the orthorhombic Fe_3C phase [28]. After 9 h of milling, the same phases are observed as those of the milled powder for 6 h. One also notes that the broad peak located at about 45° is probably due to the formation of a highly disordered phase that is superimposed to the crystalline phases peaks. Nevertheless, the mixing progress is evidenced by the increase of the proportions of both phosphides and carbides with increasing of the milling time, at the expense of the α-Fe and α-(Fe,Cr) ones. On further milling time (up to 90 h), the diffraction peaks profile appears to be diffused, so it is rather difficult from broad and overlapped peaks to distinguish crystalline phase, a disordered phase and a combination of both. The best refinement of the XRD patterns is obtained by considering at least four crystalline phases: tetragonal $(Fe,Cr)_3P$ type phosphide, orthorhombic type $(Fe,Cr)_3C$; hexagonal type $(Fe,Cr)_7C_3$ and orthorhombic type $(Fe,Cr)_7C_3$ carbides. All the XRD results are listed in Table 1 while refined XRD patterns of the FeCrPC powder milled for 6 h and for 90 h are reported in Figs. 2 and 3, respectively.

On the basis of the above XRD results, it is clear that the complete mixing of elemental Fe, Cr, P and C powders leads to the formation of nanocrystalline phosphides and carbides embedded in a disordered like amorphous state, above 9 h of milling. The phosphide phase Fe_2P appears after 3 h of milling, as obtained in the $Fe_{92}P_8$ powder mixture (Fig. 4) milled with high intensity (I = 9) [29], and disappears above 9 h of milling. However, the Fe_3P phosphide that appears after 6 h of milling, remains up to 90 h of milling. The carbide Fe_3C, or cementite, is formed at the initial stage of milling (after 6 h) as observed in the mechanical alloyed FeC system [10–12] independently of the C content. Thereafter, it is replaced by a $(Fe,Cr)_3C$ type carbide when the complete dissolution of the mixed elemental powders is achieved above 9 h, as evidenced by the change in the lattice parameters (see Table 1). The presence of the $(Fe,Cr)_7C_3$ type phase in the milled FeCrPC powder mixture, above 48 h of milling (rather dominant >55%), is somewhat particular, which differs from the results expected for the FeC system having lower carbon content (<15%) [11]. Indeed, Fe_7C_3 phase is formed over a wide concentration range from 29 to 50% C with much faster kinetics [30]. On the other hand, it has been established that the Fe_7C_3 phase is usually formed at higher carbon content, higher temperature and pressure and for longer milling time, according to the binary FeC alloy phase diagram [31] and MA process [10–12], respectively. Thus, the Fe_7C_3 phase was observed, by transmission electron microscopy, during the first stage of the crystallisation (T = 410 °C) of the amorphous $Fe_{77}Cr_4P_8C_{11}$ ribbons prepared by melt spinning [18]. In addition, this phase is known to contain a high density of defects with three crystallographic structures: hexagonal (type Ru_7C_3); orthorhombic and hexagonal (type Cr_7C_3)

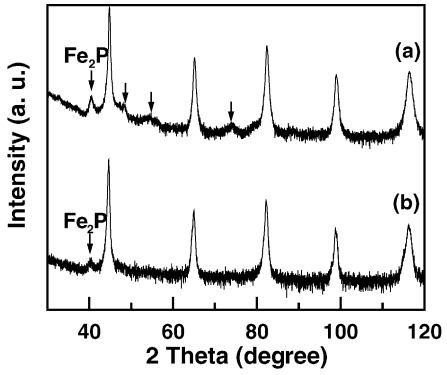

Fig. 4. Comparison of the XRD patterns of the $Fe_{92}P_8$ [29] (a) and FeCrPC (b) powders mixture, milled for 3 h.

[32]. Those structures may coexist together. Since the final product of the mechanical alloyed powders in the FeC system is affected by both the milling parameter conditions and the starting composition [12], the formation of the $(Fe,Cr)_7C_3$ type carbide in a short milling time (48 h) comparatively to that of the FeC system [10–12], is due to (i) the milling intensity ($I = 7$); (ii) the powder to ball weight ratio (2/35) and (iii) the starting elemental powders nature. In summary, since the final milling product contains only (Fe,Cr) phosphides and (Fe,Cr) carbides, the FeCrPC powder mixture can be thus described as a pseudo-ternary (Fe,Cr)PC alloy.

Mössbauer spectra of mechanically alloyed $Fe_{77}Cr_4P_8C_{11}$ powders, as shown in Fig. 5, exhibit a highly complex hyperfine profile especially for longer milling times. The hyperfine structure is strongly dependent on milling time with a progressive asymmetrical and important broadening of the sextet lines and the emergence of a quadrupolar component and low hyperfine field contributions, due to the formation of carbides and phosphides as observed by XRD. After 3 h of milling, the Mössbauer spectrum is consistent with a sextuplet related to the unreacted α-Fe (86%), a broad magnetic sextet with a relative fraction of about 6% and a paramagnetic component. These two late contributions can be considered as the disordered like amorphous fraction. The paramagnetic doublet that contains 8% of iron is due to the phosphide site. In effect, a similar paramagnetic doublet has been observed in the $Fe_{92}P_8$ powder milled for the same time [29] as shown in Fig. 6. From its hyperfine parameters values: the isomer shift, IS, and the quadrupolar splitting, QS, it is quite obvious that the phosphide obtained in the $Fe_{92}P_8$ [29] and $Fe_{77}Cr_4P_8C_{11}$ powders mixtures (Table 2) have the same IS but different QS. This difference might be attributed to the high plastic deformation induced during the milling process, which is most important in the binary $Fe_{92}P_8$ milled powders as evidenced

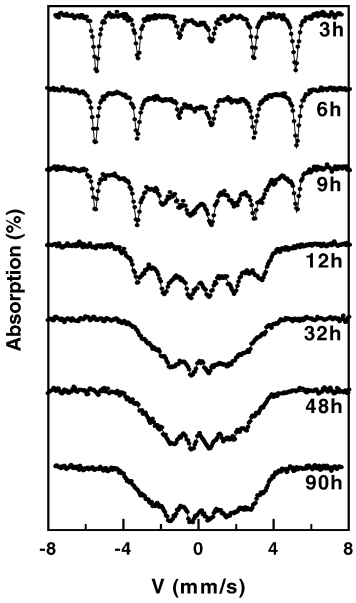

Fig. 5. Mössbauer spectra of the milled powders, taken at 300 K.

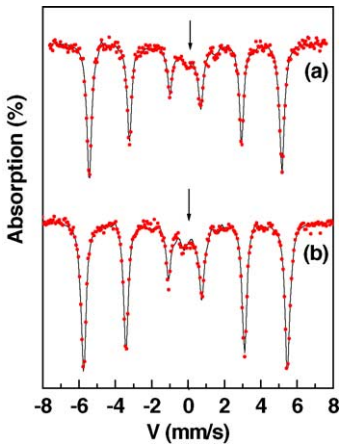

Fig. 6. Comparison of the Mössbauer spectra, taken at 300 K, of the $Fe_{92}P_8$ [29] (a) and quaternary FeCrPC (b) powders mixture, milled for 3 h.

by the existence of two α-Fe components having higher hyperfine magnetic fields ($B_1 = 35.8$ T and $B_2 = 34.6$ T). Those features arise from a very distorted structure because of the used milling conditions especially the milling intensity ($I_{FeP} = 9 > I_{FeCrPC} = 7$) and the nature of the starting elemental powders. On the other hand, knowing that: (i) both FeP and Fe_2P phosphides are paramagnetic at room temperature [33]; (ii) the obtained IS value of the phosphides falls into the same range as that of the FeP and Fe_2P phases (Table 2) and (iii) the QS value is close to that of FeP phase but greater than that of Fe_2P phase, one can thus assume that the obtained hyperfine parameters can be attributed to a non-stoichiometric phosphide phase Fe_xP with $1 < x < 2$, which is not yet known, to our knowledge.

For 6 h of milling, the disordered like amorphous fraction increases at the expense of the α-Fe component and reaches a relative proportion of about 47%. After 9 h of milling, one observes the emergence of a broad lines component in the centre of the Mössbauer spectrum with a significant decrease of the α-Fe component area, as well as the increase of the disordered amorphous like fraction. For 12 h of milling, all elemental powders are mixed at the atomic level. This is confirmed by the shape of the Mössbauer spectrum which has changed drastically. Further milling time up to 32 h leads to the disappearance of the paramagnetic doublet and thus to the formation of a magnetic disordered amorphous like state. In fact, the shape of the Mössbauer spectrum looks like that obtained for the amorphous FeC system [34] and amorphous FePC alloy [35] prepared by conventional techniques. The

Table 2
Hyperfine parameters of the paramagnetic doublet phosphide: IS and QS correspond to isomer shift (respect to α-Fe at 300 K) and quadrupolar splitting, respectively

	IS (mm/s)	QS (mm/s)	Prop (%)
$Fe_{92}P_8$ powder mixture	0.43	0.92	9
$Fe_{77}Cr_4P_8C_{11}$ powder mixture	0.43	0.66	8
FeP phase [33]	0.32	0.65	–
Fe_2P phase [33]	0.60	0.43	–

Table 3
Hyperfine parameters deduced from the fitting of the Mössbauer spectrum of the FeCrPC powder mixture milled for 90 h: IS, QS, 2ε, B_{hf} and Γ correspond to isomer shift (respect to α-Fe at 300 K), quadrupolar splitting, quadrupolar shift, hyperfine field and line width, respectively

Phases	Sites	B_{hf} (Tesla) (±0.8)	IS (mm/s) (±0.05)	QS or 2ε (mm/s) (±0.05)	Γ (mm/s) (±0.05)	Proportion (%) (±2)
ε'-$Fe_{2.2}C$ type carbide	Doublet	0	0.26	0.793	0.52	8
Disordered like amorphous phase	Site I	9.2	0.44	−0.27	0.58	19
	Site II	10.7	0.13	0.46	0.36	6
$(Fe,Cr)_7C_3$ type carbide	Site III	16.5	0.27	0.29	0.56	45
	Site IV	21.6	0.25	−0.17	0.68	11
$(Fe,Cr)_3P$ type phosphide	Site V	17.3	0.36	−0.86	0.56	11

best fitting model of the Mössbauer spectrum of the powder mixture milled for 90 h is obtained by means of six components: a paramagnetic doublet and five magnetic components (namely site I to site V, shown in Table 3). For the former, the hyperfine parameters: IS = 0.26 mm/s and QS = 0.80 mm/s are comparable to those of the superparamagnetic ε'-$Fe_{2.2}C$ carbide synthesised in a catalysis reaction at 115 °C: IS = 0.25 mm/s and QS = 0.90 mm/s [36]. For the latter, the site V can be attributed to the $(Fe,Cr)_3P$ type phase, sites III and IV to the $(Fe,Cr)_7C_3$ type phase while the lower hyperfine magnetic fields (sites I and II) can be related to the Fe atoms located within the grain boundaries or/and the amorphous rich (P,C) metalloid environments.

The milling process progress, as a function of the milling time, can be followed by the evolution of the α-Fe fraction (Fig. 7) and by the variation of both the average hyperfine magnetic field, $\langle B_{hf}\rangle$, and the isomer shift, $\langle IS\rangle$ (Fig. 8). The average hyperfine field decreases linearly up to 12 h of milling and then remains milling time independent above 32 h of milling. Meanwhile, the evolution of the average isomer shift exhibits a different behaviour. In fact, $\langle IS\rangle$ increases linearly during the first 12 h of milling, reaches a maximum value of about 0.27 mm/s after 32 h of milling and then levels off. On the basis of the above observations, one can conclude that the decrease of $\langle B_{hf}\rangle$ and the increase of $\langle IS\rangle$ during the first hours of milling are related to the mixing of the elemental powders and therefore to the diffusion of Cr, P and C into the Fe matrix. It is well established that the presence of one P and C atom in the vicinity of the Fe atom as first nearest neighbour: (i) reduces the hyperfine magnetic field, ΔB_{hf}, by about 2 [37] and 5.7 T [34], respectively, and (ii) increases the isomer shift, ΔIS, by about 0.1 mm/s [37] and 0.04 mm/s [34], respectively. While, the effect of one Cr atom situated in the first coordination shell is to reduce both the hyperfine magnetic field and the isomer shift by about 3 T and 0.2 mm/s [38], respectively. Hence, the increase of $\langle IS\rangle$ correlated to the decrease of $\langle B_{hf}\rangle$ may allow us to suppose that the effect of Cr during the alloying process, which is masked by those of P and C, can be neglected. Taking into account the variation of $\langle B_{hf}\rangle$ and $\langle IS\rangle$ with the milling time, one can suggest that the alloying process of the FeCrPC mixture leads to the formation of a disordered like amorphous state after 32 h of milling since the shape of the Mössbauer spectrum is similar to those obtained for the bulk Fe–C alloys studied as a function of C content [34] and FePC amorphous alloys [35]. The average magnetic hyperfine field of about 12.5 T is found to be lower than that obtained in the amorphous ribbons having the same composition ($\langle B\rangle$ = 20.6 T) [18]. This difference may be attributed to the thermal history of the two alloys through their elaboration conditions and especially to the MA process which leads to the nanometer scale of the crystallites size and the increase of both the microstrains and the number of atoms located in the grain boundaries (∼50%).

The hyperfine magnetic field distributions, P(B), of the disordered amorphous like phase are shown in Fig. 9 for several milling times. Above 6 h of milling, the increase of the relative fraction of the lower hyperfine fields can be attributed

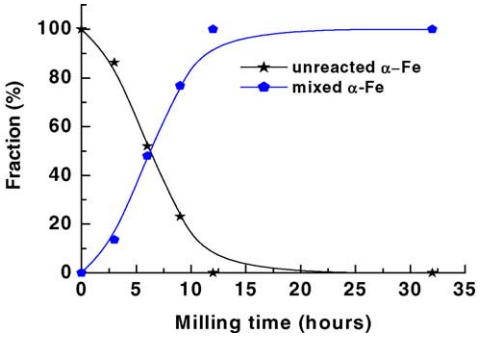

Fig. 7. Evolution of the unreacted α-Fe and mixed α-Fe fraction as a function of milling time.

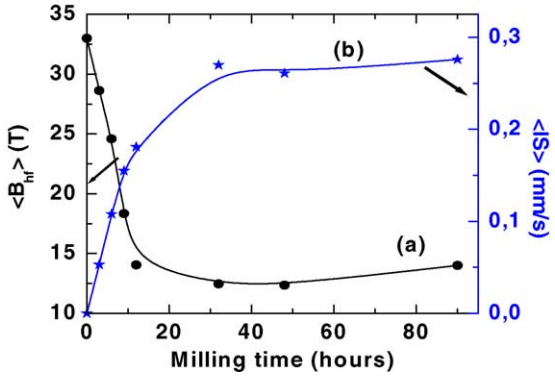

Fig. 8. Evolution of the average hyperfine parameters as a function of milling time: (a): $\langle B_{hf}\rangle$ and (b): $\langle IS\rangle$.

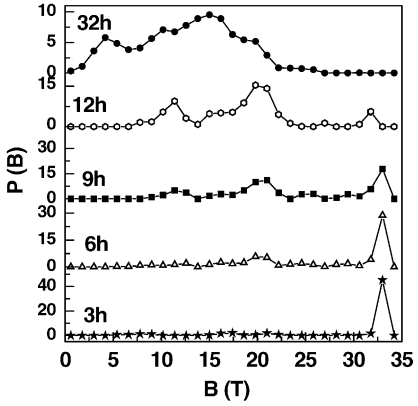

Fig. 9. Variation of hyperfine field distributions for several milling times.

to the amorphisation process which takes place as the milling time increases. After 32 h of milling, the broadening of the hyperfine field distribution, P(*B*) curve, can be due to the high lattice strains, the grain size reduction and the high density of defects and of increasing grain boundaries. The shift of the P(*B*) curve to the lower hyperfine fields is characteristic of P-based and C-based amorphous alloys and therefore related to P rich and C rich neighbourhoods in the amorphous structure. Thus, the FeCrPC powders mixture can be described as a pseudo ternary (Fe,Cr)PC.

4. Discussion

In order to understand how the alloying process of the quaternary FeCrPC powders mixture occurs during MA, MS measurements have been used jointly to XRD since their patterns are not adequate and conclusive enough to determine if the phase only results of fine-grained structures with grain boundaries or contains small crystallites embedded in an amorphous matrix. Summarizing the structural investigations, one can describe the mechanism of formation of the FeCrPC alloy by three stages as following:

Stage I: Up to 12 h of milling and corresponding to the complete mixing of all elemental powders. During this stage, the formation of α-(Fe,Cr), Fe_xP ($1 < x < 2$), Fe_3P and Fe_3C phases is certainly due to the separate alloying of Cr, P and C with Fe powders, according to their mixing enthalpy. In fact, it seems that the attraction Cr–P is rather moderate [39], whereas the Cr forms several types of carbides, as usual. It is well established that:

1. The reaction between Fe and Cr is always observed in the early stage of milling because of the negative mixing enthalpy ($\Delta H_{mix} = -1$ kJ/mole) and their bcc structures and similar lattice parameters. Thereby, the α-(Fe,Cr) phase is formed from the beginning of the milling process;
2. The appearance of the paramagnetic phosphide phase, Fe_xP type, in the early stage of milling (after 3 h) might arise from the phosphorous properties. Indeed, it is well established, that the presence of Cr in steels favors the P segregation at the grain boundaries, while its concentration is C content dependent [39]. It thereby increases when the global content of C decreases. On the other hand, P behaves generally as a stabiliser of the amorphous structure, but by itself it reacts with Fe to produce phosphides during the first stages of the MA process [40]. Also, the low melting temperature of P (∼250 °C) combined to the high energy collision due to the large amount of plastic deformation and sliding, leads to local melting which favours thus the alloying of Fe and P. It consequently originates the formation of P rich-(Fe, P) environments as evidenced by the paramagnetic doublet in the Mössbauer spectrum which is attributed to the Fe_xP ($1 < x < 2$) phosphide phase. Thus, it seems that this latter has the same crystalline structure than the Fe_2P phase as revealed by the XRD. The Fe_3P phosphide phase appears after 6 h of milling and remains for larger milling duration where it is then replaced by a $(Fe,Cr)_3P$ phosphide after a total mixing of the elemental powders Fe, Cr, C and P;
3. The formation of the Fe_3C carbide, after 6 h of milling, is obvious according to the binary Fe–C diagram phase. Indeed, it is well established that the cementite, Fe_3C, is metastable and is obtained for lower carbon content (less than 6.7%) at lower temperatures. The high diffusivity of C into the bcc Fe matrix is due to its small atomic radius and because it forms interstitial solid solution.

Stage II: Formation of a disordered amorphous like $Fe_{77}Cr_4P_8C_{11}$ alloy. Further milling (up to 32 h) leads to the amorphisation through either the diffusion-controlled reaction or by the defect-induced decomposition of the nanocrystalline intermediate products. This hypothesis may be confirmed by the disappearance of the paramagnetic Fe_xP doublet.

Stage III: Recrystallisation of the disordered amorphous like state. The appearance of new carbides such as the paramagnetic doublet ε'-$Fe_{2.2}C$ phase as well as the $(Fe,Cr)_7C_3$ type phase, above 32 h of milling, can be related to the recrystallisation of the disordered amorphous like phase, since the presence of large surface area of the mechanically milling powder particles implies a large amount of energy being stored in the milled particles. Also, the large number of defects introduced through plastic deformation allows significant diffusion to take place at room temperature. In addition, the slight heating effect due to the transfer of kinetic energy from the highly energetic ball charge enhances and sustains the diffusion process.

5. Conclusion

Amorphisation by high energy ball milling of elemental powders with the overall composition $Fe_{77}Cr_4P_8C_{11}$ has been followed as a function of milling time by XRD and MS. Initial steps in the alloying process are driven by the presence of α-Fe, α-(Fe,Cr), Fe_xP ($1 < x < 2$), Fe_3P and Fe_3C phases

during the first 9 h of milling which might arise from separate mixing and/or segregation of phosphides and carbides. Over 12 h of milling, the complete mixing of all elemental powders is reached and then leads to the formation of the disordered amorphous like state after 32 h of milling. Further milling gives rise to the formation of phosphides $(Fe,Cr)_3P$ type phase, a dominant $(Fe,Cr)_7C_3$ type phase in addition to the paramagnetic carbide ε'-$Fe_{2.2}C$ phase embedded in the amorphous matrix.

Acknowledgement

The authors are grateful to Anne Marie MERCIER from the Laboratoire des Fluorures, Université du Maine-Le Mans, France for the XRD measurements.

References

[1] R.B. Schwarz, C.C. Koch, App. Phys. Lett. 49 (1986) 146.
[2] R.B. Schwarz, R.R. Petrich, C.K. Saw, J. Non Cryst. Solids 76 (1985) 281.
[3] C.C. Koch, O.B. Cavin, C.G. McKamey, J.O. Scarbrough, Appl. Phys. Lett. 43 (1983) 1017.
[4] C. Suryanarayana, F.H. Fores, J. Mater. Res. 5–9 (1980) 1880.
[5] L. Takacs, Nanostruct. Mater. 2 (1993) 241.
[6] J.M.R. Génin, Metall. Trans. A 18 (1987) 1371.
[7] O.N.C. Uwakweh, J.Ph. Bauer, J.M.R. Génin, Metall. Trans. A 21 (1990) 589.
[8] F.E. Fujita, T. Masumoto, M. Kitaguchi, M. Ura, Jpn. J. Appl. Phys. 16 (1977) 1731.
[9] C.G. Schon, H.R. Rechenberg, H. Goldenstein, Scripta. Metall. Mater. 29 (1993) 1483.
[10] T. Tanaka, S. Nasu, K.N. Ishihara, P.H. Shingu, J. Less-Common Met. 171 (1991) 237.
[11] G. Le Caër, P. Matteazzi, Hyperfine Interact. 66 (1991) 309.
[12] S.J. Campbell, G.M. Wang, A. Calka, W.A. Kaczmarek, Mater. Sci. Eng. A226 (1997) 75.
[13] D. Basset, P. Matteazzi, F. Miani, Mater Sci. Eng. A168 (1993) 149.
[14] G.M. Wang, A. Calka, S.J. Campbell, W.A. Kaczmarek, Mater. Sci. Forum 179–181 (1995) 201.
[15] C. Djega-Mariadassou, P. Rougier, J.L. Dormann, H. Kadiri, A. Berrada, Hyperfine Interact. 45 (1989) 343.
[16] H. Kadiri, C. Djega-Mariadassou, P. Rougier, J.L. Dormann, A. Berrada, P. Renaudin, J. Physique C8 49 (1988) 1371.
[17] J. Tan, Y.F. Gao, G.D. Liu, C.L. Zhang, T. Liu, R.Z. Ma, J. Magn. Magn. Mater. 164 (1996) 211.
[18] B. Bouzabata, S. Alleg, J. Alloys Compd. 178 (1992) 117.
[19] E. Hellstern, L. Schultz, Mater. Sci. Eng. 97 (1988) 39.
[20] T. Osagawara, A. Inoue, T. Masumoto, Mater. Sci. Forum. 88–90 (1992) 423.
[21] S. Suriñach, M.D. Baro, J. Segura, M.T. Clavaguera-Mora, N. Clavaguera, Mater. Sci. Eng. A134 (1991) 1368.
[22] T. Pradell, J. Sunõl, M.T. Clavaguera-Mora, N. Clavaguera, Mater. Sci. Forum 235–238 (1997) 233.
[23] W.F. Miao, G.S. Li, S.L. Li, J.T. Wang, Acta Phys. Sinica 42 (1992) 924.
[24] L. Lutteroti, S. Matthies, H.R. Wenk, Proceeding of the Twelfth International Conference on Textures of Materials (ICOTOM-12) 1 (1999) 1599.
[25] F. Varret, J. Teillet, unpublished Mosfit program, Université du Maine, France.
[26] B. Carlsson, M. Gölin, S. Rundqvist, J. Solid State Chem. 8 (1973) 57.
[27] P. Thadani, L.E. Toth, J. Zbasnik, J. Phys. Chem. Solids 36 (1975) 987.
[28] F.H. Herbstein, J. Smuts, Acta Cryst. 17 (1964) 1331.
[29] S. Alleg, F.Z. Bentayeb, N. Bensebaa, Communication at INCOME 2003, September 7–11, 2003, Braunschweig, Germany.
[30] P. Matteazzi, G. Le Caër, J. Am. Ceram. Soc. 74 (1991) 1382.
[31] T.B. Massalski, H. Okamoto, P.R. Subrainanian, L. Kaeprzak, Binary Alloy Phase Diagram, ASM, Metals Park, OH, 1990.
[32] R. Fruchart, J.P. Senateur, J.P. Bouchaud, A. Michel, C.R.A.S. Paris 260 (1965) 913.
[33] R. Wappling, L. Häggströem, S. Rundqvist, E. Karlsson, J. Solid State Chem. 3 (1971) 276.
[34] E. Bauer-Grosse, G. Le Caër, Philos. Mag. B. 56 (1987) 485.
[35] C.C. Tsuei, G. Longwort, S.C.H. Lin, Phys. Rev. 170 (1968) 603.
[36] Yu.V. Maksimov, I.P. Suzdalev, R.A. Arents, S.M. Loktev, Kinet. Catal. 15 (1974) 1144.
[37] M. Maurer, M.C. Cadeville, J.P. Sanchez, J. Phys. F: Met. Phys. 9 (1979) 271.
[38] S.M. Dubiel, G. Inden, Z. Metallkde 78 (1987) 544.
[39] M. Guttman, D. McLean, Interfacial segregation, W.C. Johnson, J.M. Blakely (Eds.), ASM, Metals Park, OH, 1979, p. 251.
[40] R.A. Mulford, C.J. McMahon Jr., D. Pope, H.C. Feng, Metal. Trans. 7A (1976) 1183.